Supporting Information for

High surface activity of Fe-doped NiCoP for hydrogen evolution reaction

Shifan Zhu,[ab] Yixue Xu,[ab] Dong Li,[ab] Lili Song[c] and Yuqiao Wang*[ab]

[a] Research Center for Nano Photoelectrochemistry and Devices, School of Chemistry and Chemical Engineering, Southeast University, Nanjing 211189, China.

[b] Yangtze River Delta Carbon Neutrality Strategy Development Institute, Southeast University, Nanjing 210096, China

[c] School of Chemistry and Materials Science, Nanjing Normal University, Nanjing 210023, China

*Corresponding author. E-mail: yqwang@seu.edu.cn (Y. Wang)

DFT Calculation and Experimental Section

DFT Calculation: The theoretical calculations were performed based on density functional theory (DFT) using the Vienna ab initio simulation package (VASP). The ion-electron interactions were estimated by the projected augmented wave pseudopotential. The exchange-correlation energy was determined by Perdew-Burke-Ernzerhof functional based on the generalized gradient approximation. The slab models were based on the (111) plane of NiCoP and a vacuum layer of 15 Å was applied to exclude interactions in nonperiodic directions. The energy cutoff of 480 eV and Monkhorst-Pack k-points of 3×3×1 were employed to optimize the slab models and calculate the change of Gibbs free energy. The ionic force and energy convergence were set as 0.02 eV $Å^{-1}$ and 10^{-6} eV, respectively. The adsorption energy of H^* (ΔE_1) and H_2O (ΔE_2) could be calculated as following:

$$\Delta E_1 = E_{H^*} - (E^* + \frac{1}{2}E_{H_2}) \quad (1)$$

$$\Delta E_2 = E_{H_2O^*} - (E^* + E_{H_2O}) \quad (2)$$

Where E_{H^*} is the surface adsorption energy of hydrogen on the catalyst, E^* is the energy of catalyst, E_{H_2} is the formation energy of H_2, $E_{H_2O^*}$ is the surface adsorption energy of H_2O on the catalyst, E_{H_2O} is the energy of H_2O.

The Gibbs free energy for H^* adsorption was determined by following equation:

$$\Delta G_{H^*} = \Delta E + \Delta E_{ZPE} - T\Delta S \quad (3)$$

Where ΔE_{ZPE} and ΔE represent the differences in the zero-point energy and total energy difference between the reactant and product models in each step, ΔS is the entropic contribution.

Preparation of Fe-NiCoP: Firstly, Ni foam substrate was cleaned in 3.0 M HCl and washed with deionized water and ethanol for three times. $Ni(NO_3)_2 \cdot 6H_2O$ (4 mmol), $Co(NO_3)_2 \cdot 6H_2O$ (2 mmol), $Fe(NO_3)_3 \cdot 9H_2O$ (2 mmol), $NH_4F \cdot 6H_2O$ (8 mmol) and urea (20 mmol) were dissolved in 60 mL deionized water under stirring for 30 mins to form a homogeneous solution. The solution was transfered into 100 mL Teflon-lined stainless autoclave with a piece of 3×4 cm Ni foam. The autoclave was remained at 120 ℃ for 9 h. Fe-NiCo hydroxide precursor was obtained after drying at 60 ℃ for 8 h under vacuum. Then, the phosphorization process of Fe-NiCo precursor was conducted by using NaH_2PO_2 (4 mmol) as the phosphorus source in a tube furnace at 300 ℃ for 2 h under Ar_2 atmosphere with a heating rate of 5 ℃ min^{-1}. NiCoP was prepared according to the above method without $Fe(NO_3)_3 \cdot 9H_2O$. All the chemicals were analytical grade without further purification.

Characterizations: The morphologies and microstructure were characterized by scanning electron microscopy (SEM, Inspect F50, FEI) and transmission electron microscopy (TEM, F200X, Talos). The crystal structure was analyzed by X-ray diffraction (XRD, Ultima IV, Rigaku) using Cu-Kα radiation (λ = 1.54 Å). The X-ray photoelectron spectroscopy (XPS, Thermo ESCALAB 250XI) was used to analyze the surface chemical states.

Electrochemical measurements: The electrochemical measurements were performed on the electrochemical workstation (CHI 760E) using a three-electrode cell in 1M KOH. The Fe-NiCoP, graphite rod, and saturated calomel electrode (SCE) were used as the working electrode, counter electrode, and reference electrode, respectively. The Linear sweep voltammetry (LSV) was measured at the scan rate of 2 mV s^{-1}. The Tafel slope was calculated according to the curves of the overpotential versus the logarithm of current density. All potentials were converted to a reversible hydrogen electrode (RHE) using the equation: $E_{RHE} = E_{SCE} + 0.059pH + 0.241$. The electrochemical impedance spectroscopy (EIS) was measured in the frequency range of 0.01 Hz ~ 10^5 Hz at the amplitude of 5 mV. The electrochemical active surface area ($ECSA$) was calculated using the equation: $ECSA = \frac{C_{dl}}{C_s}$, where C_{dl} is the double layer capacitance calculated from cyclic voltammetry (CV) curves at different scan rates, C_s represents the general specific capacitance (0.04 mF cm^{-2}). The HER turnover frequency (*TOF*) could be calculated according to the following equation:[1-3]

$$TOF = \frac{J \times N_A}{2n \times F \times ECSA} \qquad (4)$$

where J is the current density, N_A is the Avogadro's number (6.02×10^{23}), n is the number of active sites (2.02×10^{15} cm^{-2}), F is the Faraday constant (96485 C mol^{-1}), and $ECSA$ is the electrochemical active surface area.

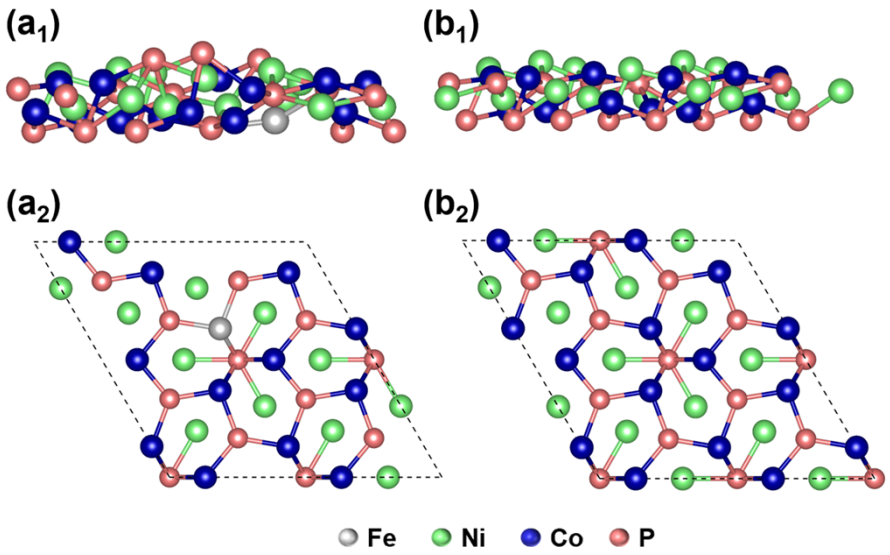

Fig. S1 Calculated models of (a_1) Fe-NiCoP and (b_1) NiCoP. H* adsorption models of (a_2) Fe-NiCoP and (b_2) NiCoP.

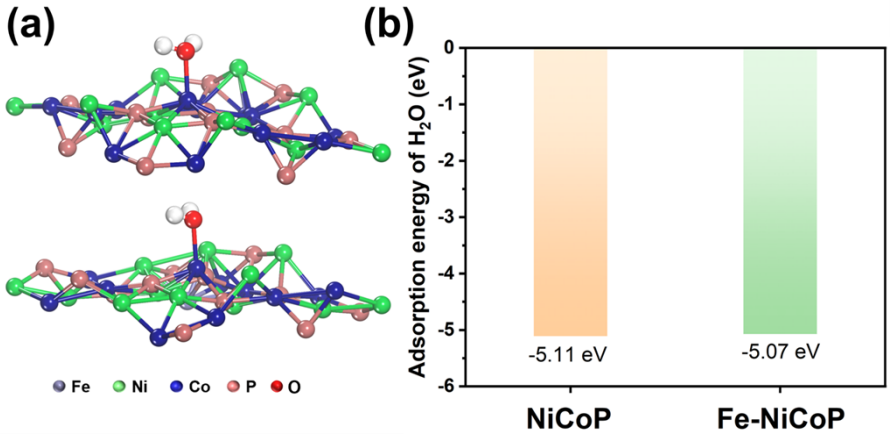

Fig. S2 (a) H_2O adsorption models of NiCoP and Fe-NiCoP. (b) H_2O adsorption energy.

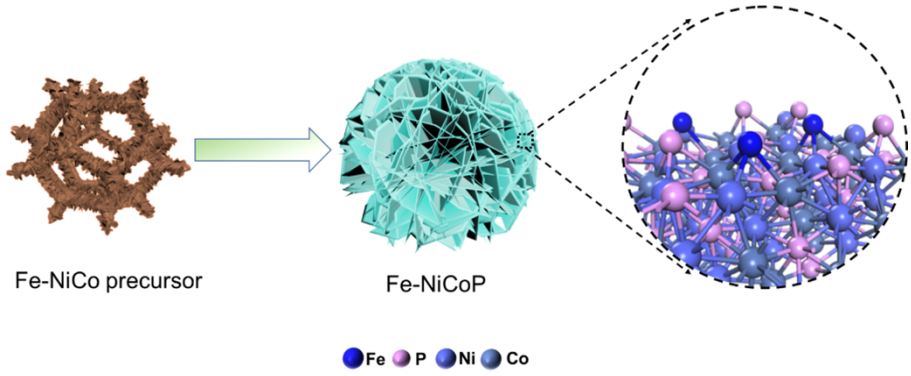

Fig. S3 Schematic illustration of the fabrication process of Fe-NiCoP.

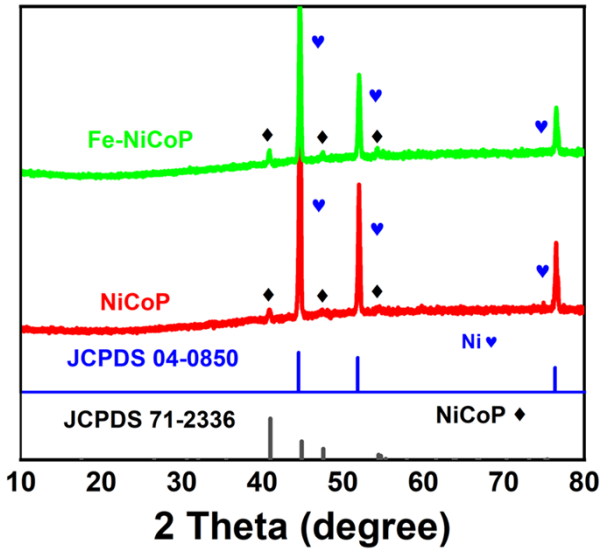

Fig. S4 XRD patterns of Fe-NiCoP and NiCoP.

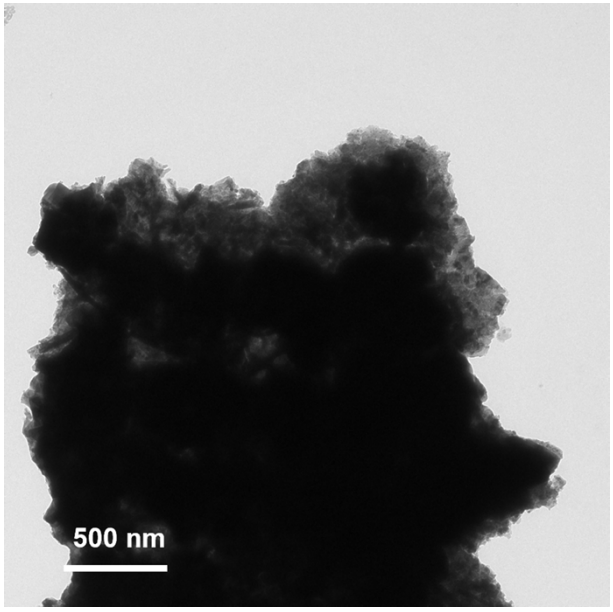

Fig. S5 TEM image of Fe-NiCoP.

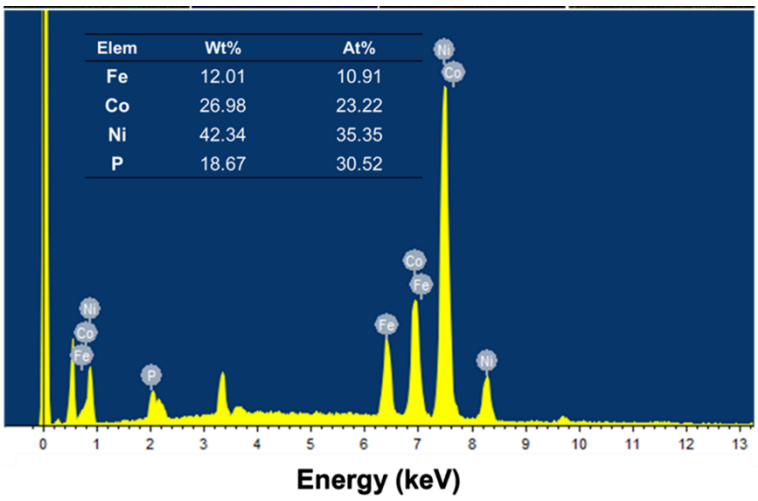

Fig. S6 The energy dispersive spectroscopy mapping of Fe-NiCoP.

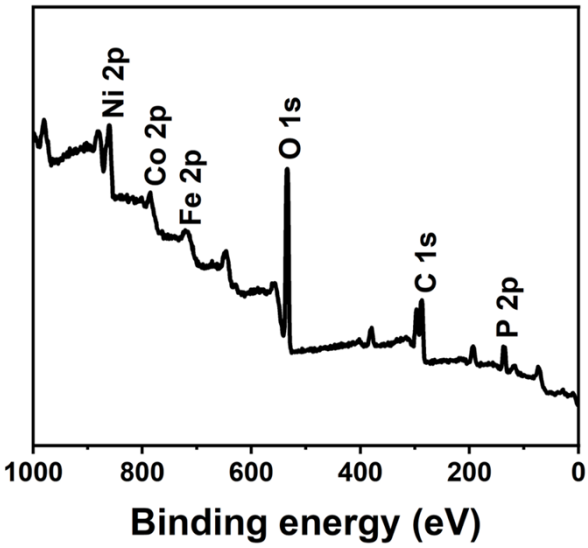

Fig. S7 XPS survey profile of Fe-NiCoP.

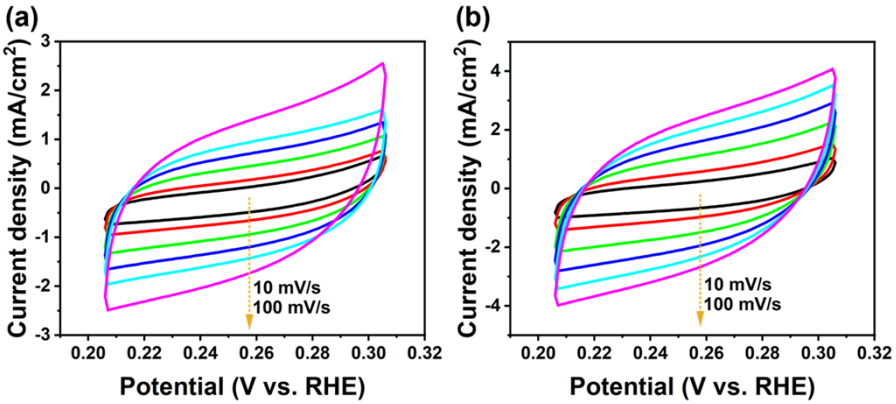

Fig. S8 Cyclic voltammetry curves of (a) NiCoP and (b) Fe-NiCoP.

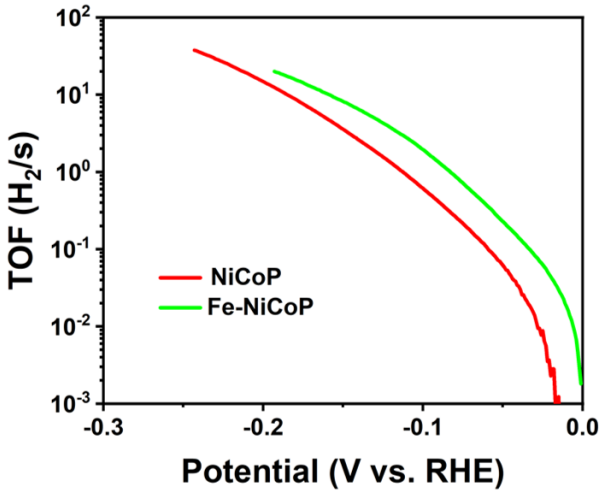

Fig. S9 Comparison of TOF values of NiCoP and Fe-NiCoP.

Table S1 Parameters of the theoretical models

Samples	a (Å)	b (Å)	c (Å)	α°	β°	γ°
NiCoP	11.6088	11.6088	3.3331	90	90	120
Fe-NiCoP	11.6297	11.6297	3.3313	90	90	120

Table S2 Comparison of HER activity with other reported catalysts

Materials	Electrolytes	Overpotential (mV, 10 mA/cm^2)	Tafel slope (mV/dec)	TOF (s^{-1})	Ref.
S-NiCoP	1 M KOH	102	63.3	0.024@100 mV	1
Ce-CoMoP/MoP	1 M KOH	188	72	0.082@200 mV	4
Fe-CoP	1 M KOH	115	72	/	5
$Ni(OH)_2/MoS_2$	1 M KOH	227	105	6@300 mV	6
CoP/ZIF-67	1 M KOH	154	85.1	0.0477@180 mV	7
C-CoP_4	1 M KOH	123	131	/	8
$FeCoP_2$@NPPC	1 M KOH	150	79	/	9
NiFeP@C	1 M KOH	160	75.8	/	10
CoFe/N_H-C NS	1 M KOH	230	97.5	/	11
Fe-NiCoP	1 M KOH	84	67.8	1.95@100 mV	This Work

Table S3 The simulated data from EIS curves

Samples	R_s/Ω	R_{ct}/Ω
NiCoP	1.46	3.61
Fe-NiCoP	1.36	2.86

References

1 Y. Qi, L. Zhang, L. Sun, G. Chen, Q. Luo, H. Xin, J. Peng, Y. Li and F. Ma, *Nanoscale*, 2020, **12**, 1985-1993.

2 Y. Zhang, K. E. Arpino, Q. Yang, N. Kikugawa, D. A. Sokolov, C. W. Hicks, J. Liu, C. Felser and G. Li, *Nat. Commun.*, 2022, **13**, 7784.

3 L. Li, Z. Qin, L. Ries, S. Hong, T. Michel, J. Yang, C. Salameh, M. Bechelany, P. Miele, D. Kaplan, M. Chhowalla and D. Voiry, *ACS Nano*, 2019, **13**, 6824-6834.

4 T. Chen, Y. Fu, W. Liao, Y. Zhang, M. Qian, H. Dai, X. Tong and Q. Yang, *Energy Fuels*, 2021, **35**, 14169-14176.

5 M. Qian, X. Tong, Z. Chen, W. Liao, Y. Fu, H. Dai, Q. Yang and T. Chen, *Ionics*, 2022, **28**, 2301-2307.

6 G. Zhao, Y. Lin, K. Rui, Q. Zhou, Y. Chen, S. X. Dou and W. Sun, *Nanoscale*, 2018, **10**, 19074-19081.

7 Y.-L. Meng, J. Tang, X. Chen, Z.-Y. Niu, Y.-H. Zhao, Y. Pan, X.-F. Wang, X.-Z. Song and Z. Tan, *Inorg. Chem. Commun.*, 2021, **134**, 109058.

8 C. Wang, G. Sui, D. Guo, J. Li, L. Zhang, S. Li, J. Xin, D.-F. Chai and W. Guo, *J. Colloid Interf. Sci.*, 2021, **599**, 577-585.

9 Y.-N. Wang, Z.-J. Yang, D.-H. Yang, L. Zhao, X.-R. Shi, G. Yang and B.-H. Han, *ACS Appl. Mater. Interfaces*, 2021, **13**, 8832-8843.

10 Q. Kang, M. Li, J. Shi, Q. Lu and Feng Gao, *ACS Appl. Mater. Interfaces*, 2020, **12**, 19447-19456.

11 S. Chen, F. Bi, K. Xiang, Y. Zhang, P. Hao, M. Li, B. Zhao and X. Guo, *ACS Sustainable Chem. Eng.*, 2019, **7**, 15278-15288.